

LETTERS

In-Situ Analysis of Valence Conversion in Transition Metal Oxides Using Electron Energy-Loss Spectroscopy

Zhong L. Wang,^{*,†} Jin S. Yin,[†] Wei Dong Mo,[‡] and Z. John Zhang[§]

School of Materials Science and Engineering, and School of Chemistry and Biochemistry, Georgia Institute of Technology, Atlanta, Georgia 3033-0245, and Department of Physics and Chemistry, Xian Air Force Engineering Institute, Xian 710038, China

Received: May 14, 1997; In Final Form: July 15, 1997[⊗]

Transition metal oxides are a class of materials that are vitally important for developing new materials with functionality and smartness. The unique properties of these materials are related to the presence of elements with mixed valences. The measurement of cation valence states can be performed using X-ray photoelectron spectroscopy and other chemical techniques, but these techniques are suitable only for a large quantity of specimens and the measured results are an average over all of the surface layer or the entire volume. For today's research in the nanoera, it is important to determine the valence states from a region as small as a nanoparticle. In this Letter, we report the success of using electron energy-loss spectroscopy, attached to a transmission electron microscope, to measure the valence states in the Co–O and Mn–O systems at a spatial resolution of 20–70 nm. The reliability and sensitivity of the technique are demonstrated in reference to the composition curves and the electron diffraction data recorded in-situ during the reductions of Co₃O₄ and MnO₂ and during the phase transformation in a solid solution of Fe₂O₃ and Mn₂O₃ as well.

Transition and rare earth metal oxides are the fundamental ingredients for many advanced and functional materials with potential applications such as sensors, actuators, and transducers.¹ The unique properties of these materials are often related to the presence of mixed valence cations and oxygen vacancies.² La_{1-x}Ca_xMnO_{3-y}, a material that has been found to exhibit the colossal magnetoresistance effect, is a typical example. In this compound, the local residual charge induced by partially substituting trivalent La cation with divalent Ca cation is balanced largely by the valence state conversion of Mn from 3+ to 4+ and/or by the creation of oxygen vacancies. The presence of mixed Mn³⁺ and Mn⁴⁺ in the compound is

considered to play a key role in the novel electric and magnetic properties of the material.³ The valence states of metal cations in such materials can certainly be chemically determined using the redox titration, but it is extremely hard to be performed on nanophase or nanostructured materials such as thin film materials. The wet chemistry approaches usually do not provide any spatial resolution. X-ray photoelectron spectroscopy (XPS) can provide information on the average distribution of cation valences for nanostructured materials with certain spatial resolution, but the spatial resolution is nowhere near the desired nanometer scale in nanophase-material studies.

Electron energy-loss spectroscopy (EELS), a powerful technique for materials characterization at nanometer spatial resolution, has been widely used in chemical microanalysis and the studies of solid state effects.^{4,5} In EELS, the L ionization edges of transition-metal and rare-earth compounds usually display sharp peaks at the near edge region, which are known as *white lines*. For transition metals with unoccupied 3d states, the

* To whom correspondence should be addressed. E-mail: zhong.wang@mse.gatech.edu.

[†] School of Materials Science and Engineering, Georgia Institute of Technology.

[‡] Xian Air Force Engineering Institute.

[§] School of Chemistry and Biochemistry, Georgia Institute of Technology.

[⊗] Abstract published in *Advance ACS Abstracts*, August 15, 1997.

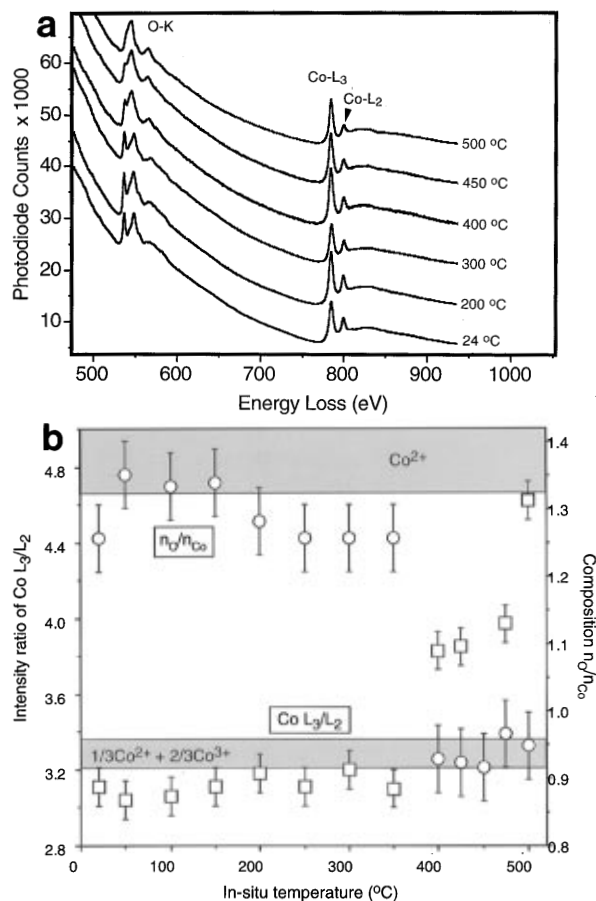


Figure 1. (a) Series of EELS spectra acquired in-situ from Co₃O₄, showing the evolution in O–K fine structure and the Co–L_{2,3} white line intensities due to the reduction of the specimen. (b) Overlapped plot of the white line intensity ratio of Co L₃/L₂ and the corresponding chemical composition of $n_{\text{O}}/n_{\text{Co}}$ as a function of the in-situ temperature of the Co₃O₄ specimen, showing the abrupt change in valence state and oxygen composition at 400 °C. The error bars are determined from the errors introduced in background subtraction and data fluctuation among spectra.

transition of an electron from a 2p state to 3d levels leads to the formation of white lines. The atomic state changes from $2p^6 3d^{(m)}$ to $2p^5 3d^{(m+1)}$ after the excitation of a 2p electron, where m stands for the number of occupied 3d states. The L₃ and L₂ lines are the transitions of $2p^{3/2}$ to $3d^{3/2} 3d^{5/2}$ and $2p^{1/2}$ to $3d^{3/2}$, respectively, and their intensities are related to the unoccupied states in the 3d bands.⁶

Numerous EELS experiments have shown that a change in valence states of cations introduces a dramatic change in the ratio of the white lines, leading to the possibility of identifying the occupation number of 3d orbitals using EELS.^{7–14} Morrison et al.¹² has applied this technique to study the valence modulation in the Fe_xGe_{1-x} alloy as a function of Ge doping. The 3d and 4d occupations of transition and rare earth elements have been studied systematically by Pearson et al.^{8,9} The reliability of this measurement has been examined for the Mn–O system in comparison to the molecular orbital calculation.¹⁰ The crystal structure of a new compound Mn_{7.5}Br₃O₁₀ has been refined in reference to the measured Mn valences,¹³ and the oxidation states of Ce and Pr have been determined in an orthophosphate material, in which the constituents of Ce and Pr are on the order of 100 ppm. Recently, oxygen vacancies in La_{0.67}Ca_{0.33}MnO_{3-δ} have been determined to be less than 2.2 at. % on the basis of the measured Mn valence,¹⁵ and the crystal structure of La_{0.5-}

Sr_{0.5}CoO_{2.25} has been quantitatively determined in reference to the valence information of Co obtained by EELS studies.^{16,17}

In this paper, EELS is applied to determine in-situ the valence state conversion in transition metal oxides. The sensitivity and reliability of the technique are demonstrated. It is shown that EELS is a powerful technique for the quantitative analysis of mixed valences in transition metal oxides at a high spatial resolution.

The EELS experiments were performed at 200 kV using a Hitachi HF-2000 transmission electron microscope equipped with a Gatan 666 parallel-detection electron energy-loss spectrometer. A Gatan TEM specimen heating stage was employed to carry out the in-situ EELS experiments, and the specimen temperature could be increased continuously from room temperature to 1000 °C. The column pressure was kept at 3×10^{-8} Torr or lower during in-situ analysis. Thus, the oxygen partial pressure near the specimen in TEM was very low, resulting in little oxidation during the experiments. The EELS spectra were acquired in the image mode at a magnification of 40–100 K, and therefore the spatial resolution was controlled at 20–70 nm depending on the size of the spectrometer entrance aperture and the image magnification. Polycrystalline powder specimens were dispersed on holey carbon grids for TEM observation. A low-loss valence spectrum and the corresponding core–shell ionization edge EELS spectrum were acquired consecutively from the same specimen region. The low energy-loss spectrum was used to remove the multiple-inelastic-scattering effect in the core-loss region using the Fourier ratio technique. Consequently, the data presented here are the results of the single scattering of electrons.

EELS analysis of the valence state is carried out in reference to the spectra acquired from standard specimens with known cation valence states.^{8–14} Since the intensity ratio of L₃/L₂ is sensitive to the valence state of the corresponding element, if a series of EELS spectra are acquired from several standard specimens with known valence states, an empirical plot of these data serves as the reference for determining the valence state of the element present in a new compound. This method has been successfully demonstrated for La_{0.5}Sr_{0.5}CoO_{2.25} and La_{0.67}Ca_{0.33}MnO_{3-y}, and the detailed experimental method is reported elsewhere.^{15,16} To establish the numerical relationship between the intensity ratio of white lines with the number of unoccupied d states, the white lines are isolated from the continuous background using the empirical method introduced by Pearson et al.⁸ This background subtraction procedures are followed consistently for all of the acquired spectra.

In-Situ Reduction of Co₃O₄ and MnO₂

For testing the sensitivity and reliability of using white line intensity to determine the valence states in mixed valence compounds, the in-situ reduction behavior of Co₃O₄ is examined first. Figure 1a shows a comparison of as-acquired EELS spectra of Co₃O₄ as a function of temperature. Three striking features are observed. First, the fine edge structure of O–K is dramatically changed when the specimen temperature is higher than 400 °C. The change of near edge structure indicates a change in the density of states in the valence band, i.e., solid state effect, which indicates a possible structural evolution. Second, since the integrated intensity of the ionization edge is proportional to the atomic concentration of the corresponding element, a decrease in O–K intensity as the temperature increases indicates a reduction in oxygen content. Finally, the relative intensity of Co–L₂ to Co–L₃ decreases as the specimen temperature increases, characterizing a change in valence state. A quantitative representation of these changes is displayed in

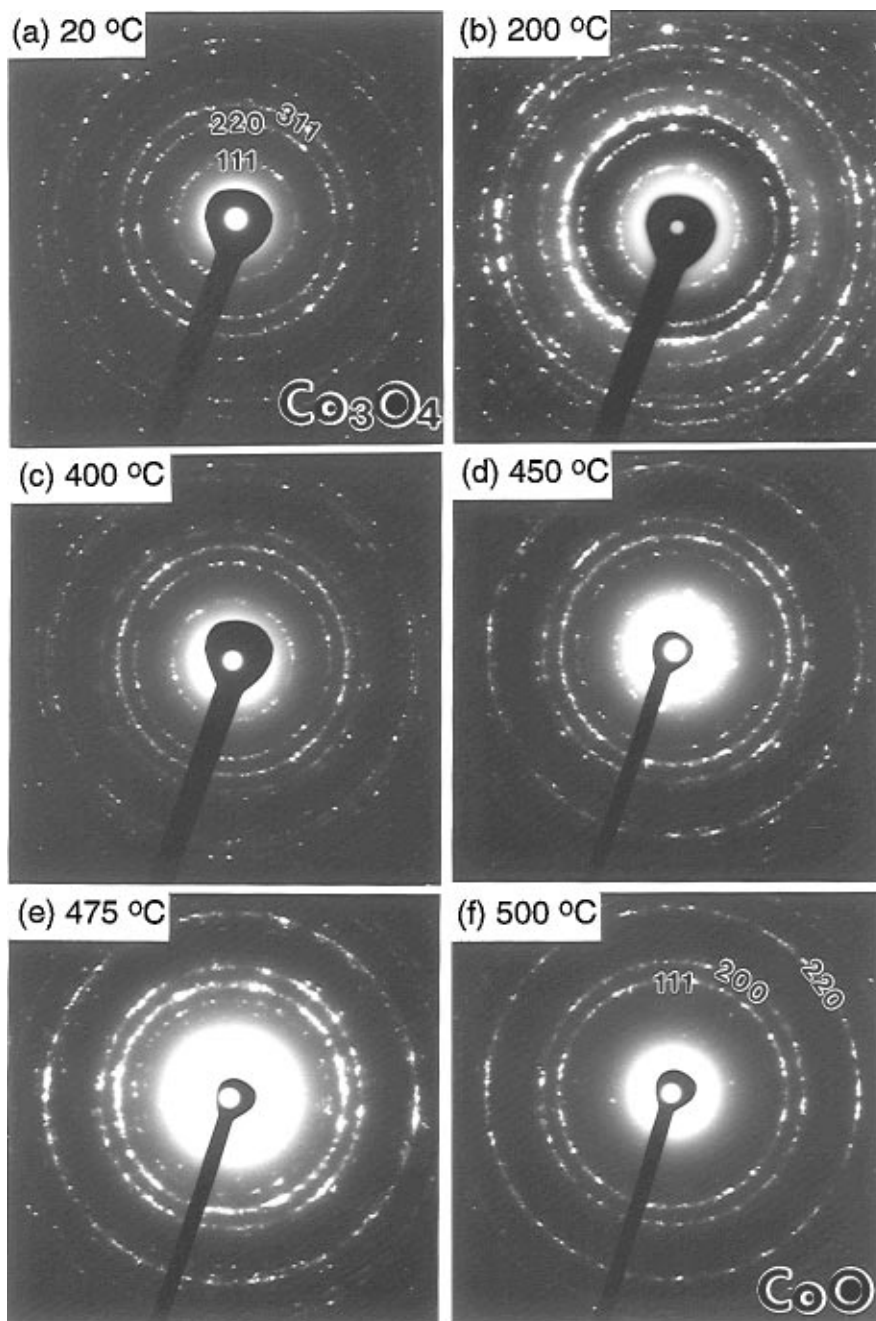


Figure 2. Series of electron diffraction patterns of the Co_3O_4 specimen recorded in-situ, showing the transformation in crystal structure above 475 °C.

Figure 1b, in which the $\text{Co } L_3/L_2$ ratio and the relative composition of $n_{\text{O}}/n_{\text{Co}}$ are plotted as a function of the specimen temperature. The specimen composition was determined from the integrated intensities of the O-K and Co-L_{2,3} ionization edges with the use of ionization cross sections calculated using the SIGMAK and SIGMAL programs.⁴ The L_3/L_2 ratios corresponding to Co^{2+} , determined from the EELS spectra of CoSO_4 and CoCO_3 at room temperature, and corresponding to $\text{Co}^{2.67+}$ obtained from Co_3O_4 are marked by shadowed bands, the widths of which represent experimental error and the variation among different compounds.¹⁶ The $\text{Co } L_3/L_2$ ratio and the composition, $n_{\text{O}}/n_{\text{Co}}$ simultaneously experience a sharp change at $T = 400$ °C. The chemical composition changes from $\text{O}:\text{Co} = 1.33 \pm 0.5$ to $\text{O}:\text{Co} = 0.95 \pm 0.5$, accompanying the change of the average valence state of Co from 2.67+ to 2+ when the temperature is above 400 °C.

To trace the evolution of crystal structure, electron diffraction patterns were recorded from the same aggregate of Co_3O_4

particles at different temperatures. The starting material is cubic Co_3O_4 with a spinel structure and a lattice constant $a = 8.083$ Å (Figure 2a). The crystal structure, Co valence states, and oxygen composition are preserved up to 400 °C. In the temperature range of 400–475 °C, the reduction process occurs and the Co valence is modified although the crystal structure still preserves the spinel type (Figure 2b–e). Soon after the temperature reaches 500 °C, the crystal structure converts to CoO of the NaCl-type ($a = 4.2667$ Å) (Figure 2f), which is certainly consistent with a composition of $\text{O}:\text{Co} = 0.95 \pm 0.5$ and the Co valence of 2+ (Figure 1b).

The second experiment is on the reduction of MnO_2 . Figure 3a shows a series of EELS spectra recorded from a single crystalline MnO_2 as the specimen temperature was increased from 24 to 500 °C. The features seen from the spectra are similar to those described above for Co_3O_4 : the reduction of the material is accompanied by a change in the valence state of Mn. A plot of composition, $n_{\text{O}}/n_{\text{Mn}}$, and white line intensity,

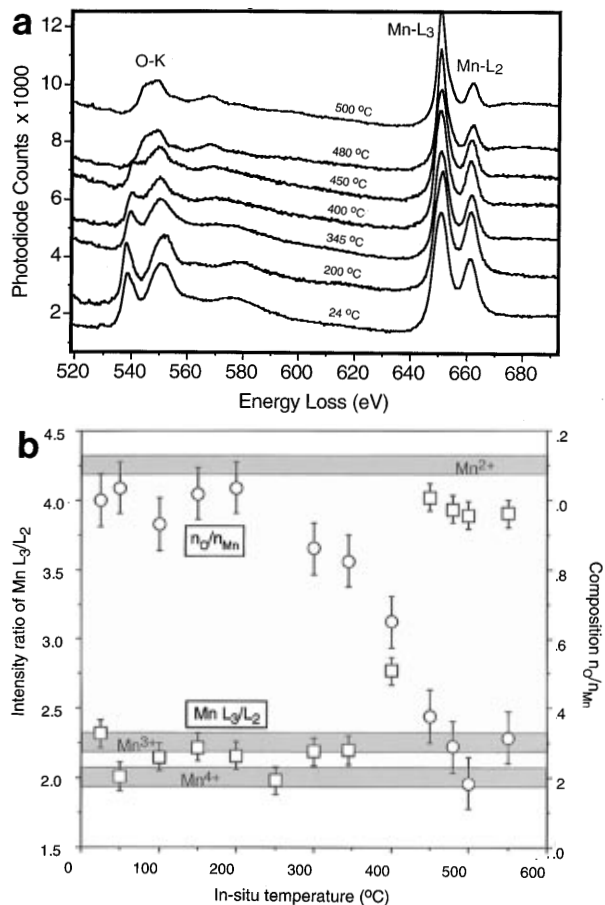


Figure 3. (a) Series of EELS spectra acquired in-situ from MnO₂, showing the evolution in O–K fine structure and the Mn–L_{2,3} white line intensities due to the reduction of the specimen. (b) Overlapped plot of the white line intensity ratio of Mn L₃/L₂ and the corresponding chemical composition of n_O/n_{Mn} as a function of the in-situ temperature of the MnO₂ specimen based on EELS spectra, showing a continuous change in Mn valence state and oxygen composition.

Mn L₃/L₂ is given in Figure 3b; the shadowed bands indicate the white line ratios for Mn²⁺, Mn³⁺, and Mn⁴⁺ as determined from the standard specimens of MnO, Mn₂O₃, and MnO₂, respectively.^{9,15} The reduction of MnO₂ occurs at 300 °C, lower than the one for Co₃O₄. As the specimen temperature increases, the O/Mn ratio drops and the L₃/L₂ ratio increases, which indicates the valence state conversion of Mn from 4+ to lower valence states. At *T* = 400 °C, the specimen contains the mixed valences of Mn⁴⁺, Mn³⁺, and Mn²⁺. As the temperature reaches 450 °C, the specimen is dominated by Mn²⁺ and the composition has O/Mn = 1.3 ± 0.5, slightly higher than that in MnO, which is consistent with the mixed valence of Mn cations and implies the uncompleted reduction of MnO₂.

In-Situ Solid State Reaction in a Fe₂O₃–Mn₂O₃ Solid Solution

EELS studies of the above two specimens have clearly illustrated the sensitivity and reliability of using the white line intensity ratio to determine the valence states of transition metal elements. To demonstrate the extensive application of this technique, EELS study of solid state reaction in an Fe₂O₃–Mn₂O₃ solid solution has been conducted. The specimen was prepared by the coprecipitation method. The aqueous solutions of FeCl₃ and MnCl₂ were first mixed, and then concentrated NaOH solution was added into the mixed solution to form precipitation. The crystallographic structure of the as-synthesized specimen was determined by X-ray and electron diffrac-

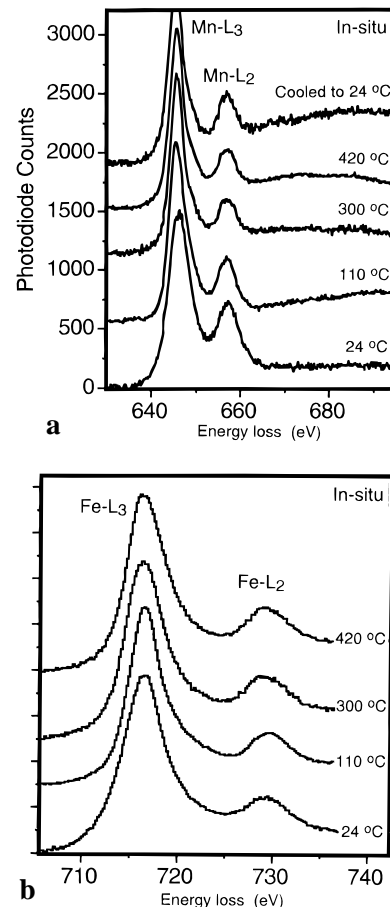


Figure 4. Single-scattering EELS spectra of (a) Mn–L_{2,3} and (b) Fe–L_{2,3} ionization edges, recorded in-situ from the solid solution of Fe₂O₃ and Mn₂O₃, showing a temperature-driven structural evolution.

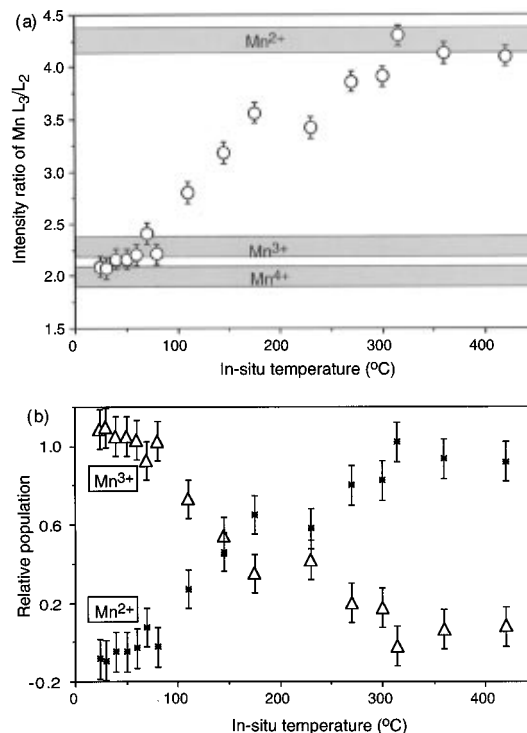


Figure 5. (a) Plot of the white line intensity ratio of Mn L₃/L₂, based on the EELS spectra recorded from the solid solution of Fe₂O₃ and Mn₂O₃, showing a slow valence conversion process due to the solid state reaction. (b) Calculated relative populations of Mn³⁺ and Mn²⁺ based on the white line intensity ratios, illustrating the valence conversion process in the reaction.

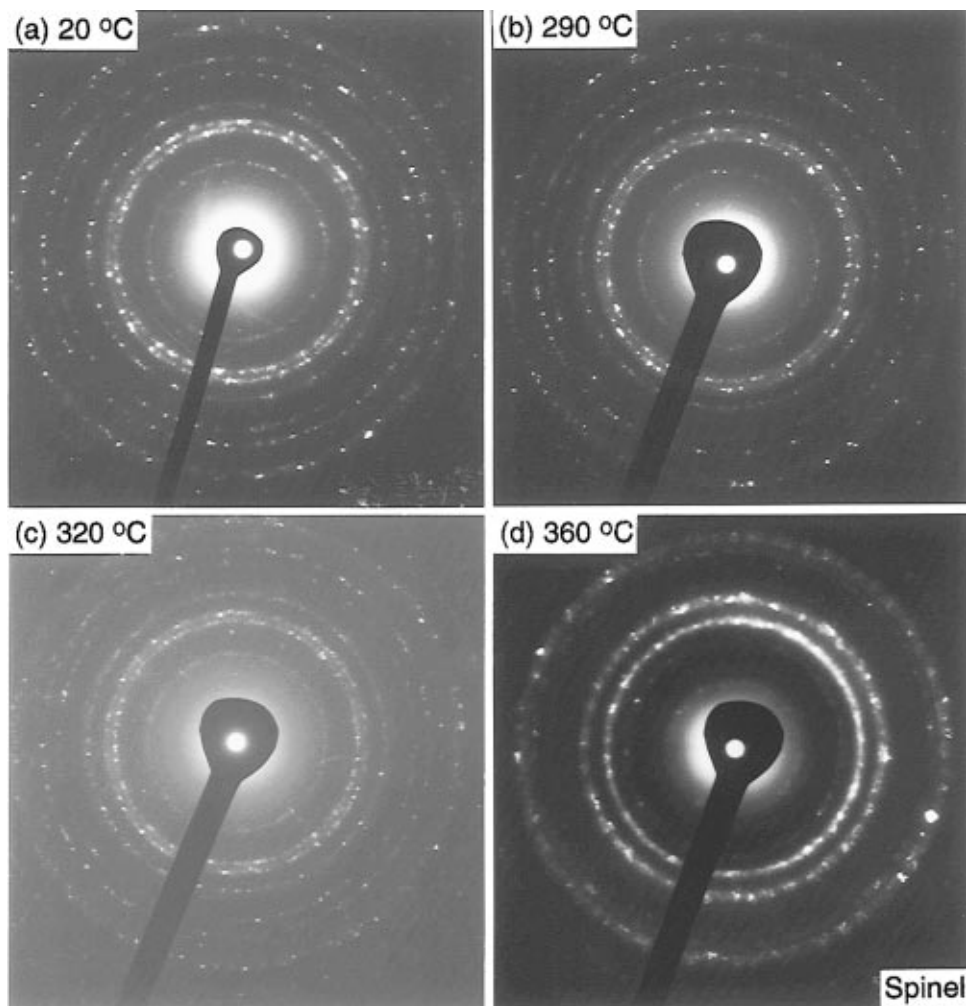


Figure 6. Series of electron diffraction patterns recorded from the solid solution of Fe_2O_3 and Mn_2O_3 , showing a sharp change in crystal structure as the temperature increases from 320 to 360 °C.

tion. The diffraction patterns showed it is a solid solution of Fe_2O_3 and Mn_2O_3 with the ratio of Fe/Mn about 2. This result is consistent with the Fe_2O_3 – Mn_2O_3 phase diagram revealing a favorable formation of a solid solution containing Mn_2O_3 from 15 to 75 mol %.¹⁸ Fe_2O_3 has a corundum structure, and Mn_2O_3 has an *C*-rare earth structure. The formation of Mn_2O_3 is rather not a surprise since it is the favorable product when the aqueous solution of MnCl_2 is added with a strong base and becomes very basic.¹⁹ The specimen shows well-dispersed nanoparticles with sizes of 5–10 nm. EELS spectra were acquired in-situ from a cluster of particles, as shown in Figure 4. It is apparent that the relative intensity of Mn– L_2 with respect to Mn– L_3 decreases as the temperature increases, indicating a change in Mn valence. However, the L_3/L_2 ratio of Fe shows little change, indicating the stable valence state of Fe^{3+} , which is reasonable since Fe^{2+} is a very unstable species. A plot of Mn L_3/L_2 is given in Figure 5a, which displays a slow variation in contrast to the sharp variation observed in Figure 3b for MnO_2 . Due to the limitation of the technique, there could be some ambiguity in distinguishing the valence state between Mn^{3+} and Mn^{4+} since the difference in L_3/L_2 ratios for Mn^{3+} and Mn^{4+} is rather small. In this case, the structural information provided by electron diffraction can resolve the uncertainty in identifying the valence state. The white line intensity, L_3/L_2 , shows almost no change at temperatures below 100 °C. It increases from 100 °C and becomes stabilized at 340 °C, which implies that the valence state of Mn transfers from 3+ to 2+ within this temperature range.

With the use of white line intensity, it is possible to determine the ratio of $\text{Mn}^{3+}/\text{Mn}^{2+}$ at different temperatures in reference to the empirical curve measured experimentally.¹⁵ A plot of the calculated relative population of Mn^{2+} and Mn^{3+} is given in Figure 5b. The valence conversion from Mn^{3+} to Mn^{2+} is apparent as the temperature increases. The conversion starts at $T \sim 90$ °C and ends at $T \sim 310$ °C.

To understand the nature of this slow evolution process, electron diffraction patterns were recorded in-situ from the same aggregation of nanoparticles, and the result is shown in Figure 6. There is no structural change for Mn_2O_3 and Fe_2O_3 at temperatures lower than 340 °C. Although Fe_2O_3 and Mn_2O_3 have different crystal structure, the diffraction rings of Fe_2O_3 are almost overlapped with those of Mn_2O_3 (the diffraction rings with significant intensities for Fe_2O_3 are $d_{(012)} = 0.368$ nm, $d_{(104)} = 0.27$ nm, $d_{(110)} = 0.252$ nm, and $d_{(006)} = 0.229$ nm and for Mn_2O_3 are $d_{(211)} = 0.384$ nm, $d_{(222)} = 0.272$ nm, $d_{(321)} = 0.251$ nm, and $d_{(400)} = 0.235$ nm).²⁰ The reflection rings of Mn_2O_3 and Fe_2O_3 are almost coincident, and the difference between them is hardly distinguishable using either electron diffraction or X-ray diffraction because of the line broadening in the spectra induced by small crystal size. As the temperature approaches 360 °C, the crystal structure is transformed into the spinel type (Figure 6d), indicating the formation of MnFe_2O_4 , which is supported by the chemical microanalysis. Since trivalent Fe cations are present in both Fe_2O_3 and MnFe_2O_4 , this solid state conversion process is also consistent with the slow increase of the L_3/L_2 ratio (Figure 5) that represents a graduate transforma-

tion of Mn^{3+} into Mn^{2+} . The kinetics of this reaction strongly depends on the specimen temperature, and the relatively low reaction temperature is possible due to the small size of the particles. The structural evolution presented here is an irreversible process. When the specimen is cooled back to 24 °C after the studies, the white line intensity ratio of Mn L_3/L_2 shows little difference from that observed at 420 °C (Figure 4). This is a direct proof that the observed phenomenon is owing to structural evolution rather than a temperature-driven reversible phase transformation.

The electron diffraction patterns displayed in Figure 6 clearly show that the structural transformation to spinel occurs in a much narrower temperature range than that of the valence state. The possible reasons are as follows. The release of oxygen is a slow process. With the increase of specimen temperature, some oxygen in the crystal structure of the nanoparticles is gradually released and anion vacancies are formed. The local charge is balanced by the valence conversion of some Mn cations from 3+ to 2+. Since the electron diffraction pattern is largely determined by the cation lattice due to their stronger scattering power than oxygen, the diffraction pattern is most sensitive to the change on the cation lattice in the crystal structure. After a substantial amount of oxygen is released, the stability of the cation lattice cannot be maintained because of the lack of the anion coordination, and a sudden transformation in the crystal structure occurs.

In conclusion, relying on the intensity ratio of white lines, the valence state of a transition metal element can be determined. The reliability of the technique is demonstrated in reference to the composition curves and electron diffraction data recorded in-situ from three different specimens. For characterizing advanced and functional materials that usually contain cations with mixed valences, this is a very powerful approach with a spatial resolution higher than any other spectroscopy techniques.

Acknowledgment. This work was supported in part by NSF Grant DMR-9632823.

References and Notes

- (1) Newnham, R. E.; G. R. Ruschau, *J. Am. Ceram. Soc.* **1991**, *74* (3), 463–480.
- (2) Wang, Z. L.; Kang, Z. C. *Functional and Smart Materials-Structural Evolution and Structure Analysis*; Plenum Press: New York, 1997.
- (3) Zener, C. *Phys. Rev.* **1951**, *82*, 403–405.
- (4) Egerton, R. F. *Electron Energy-Loss Spectroscopy in the Electron Microscope*, 2nd ed.; Plenum Press: New York, 1996.
- (5) Disko, M. M.; Ahn, C. C.; Fultz, B., Eds.; *Transmission Electron Energy Loss Spectrometry in Materials Science*; The Minerals, Metals and Materials Society: Warrendale, PA, 1992.
- (6) Krivanek, O. L.; Paterson, J. H. *Ultramicroscopy* **1990**, *32*, 313–318.
- (7) Rask, J. H.; Mine, B. A.; Buseck, P. R. *Ultramicroscopy* **1987**, *32*, 319–325.
- (8) Pearson, D. H.; Ahn, C. C.; Fultz, B. *Phys. Rev. B* **1993**, *47*, 8471–8478.
- (9) Pearson, D. H.; Fultz, B.; Ahn, C. C. *Appl. Phys. Lett.* **1988**, *53*, 1405–1407.
- (10) Kurata, H.; Colliex, C. *Phys. Rev. B* **1993**, *48*, 2102–2108.
- (11) Pease, D. M.; Bader, S. D.; Brodsky, M. B.; Budnick, J. I.; Morrison, T. I.; Zaluzec, N. J. *Phys. Lett.* **1986**, *114A*, 491–494.
- (12) Morrison, T. I.; Brodsky, M. B.; Zaluzec, N. J.; Sill, L. R. *Phys. Rev. B* **1985**, *32*, 3107–3111.
- (13) Mansot, J. L.; Leone, P.; Euzen, P.; Palvadeau, P. *Microsc., Microanal., Microstruct.* **1994**, *5*, 79–90.
- (14) Fortner, J. A.; Buck, E. C. *Appl. Phys. Lett.* **1996**, *68*, 3817–3819.
- (15) Wang, Z. L.; Yin, J. S.; Jiang, Y. D.; Zhang, J. *Appl. Phys. Lett.* **1997**, *70*, 3362–3364.
- (16) Wang, Z. L.; Yin, J. S. *Phil. Mag. B* in press.
- (17) Yin, J. S.; Wang, Z. L. In *Proceedings of the Microscopy Society of America*; Bailey, G. W., Ed.; San Francisco Press: San Francisco, CA, in press.
- (18) Mason, B. *Am. Mineral.* **1944**, *29*, 67–77.
- (19) Liang, C. C. In *Encyclopedia of Electrochemistry of the Elements*; Bard, A. J., Ed.; Marcel Dekker, Inc.: New York, 1973; p 352; Vol. 1.
- (20) From: *Selected Powder Diffraction Data for Education and Training*; International Centre for Diffraction Data: Swarthmore, PA, 1988.